Short Communication

Electrodeposition of Aluminum from AlCl₃-1-Ethyl-3-Methylimidazolium Fluoride

Dexi Wang[1,2], Xiongwei Zhong[1,3], Fengguo Liu[1,4], Zhongning Shi[1,4]*

[1] Key Laboratory for Ecological Utilization of Multimetallic Mineral (Ministry of Education), Northeastern University, Shenyang 110819, China
[2] School of Chemical Engineering Equipment, Shenyang University of Technology, Liaoyang 111003, China
[3] Department of Materials Science and Engineering, Southern University of Science and Technology, Shenzhen, 518055, China
[4] School of Metallurgy, Northeastern University, Shenyang 110819, China.
[*]E-mail: shizn@smm.neu.edu.cn

The electrodeposition of aluminum was successfully achieved in AlCl₃-1-ethyl-3-methylimidazolium fluoride (EmimF) at a potential of –0.3V (vs. Al/Al³⁺) and a temperature of 90 ℃. Cyclic voltammetry, chronopotentiometry and chronoamperometry were used to investigate the electrochemical behavior of $Al_2Cl_7^-$. Cyclic voltammetry and chronopotentiometry measurements indicate that the reduction of $Al_2Cl_7^-$ to metallic Al in AlCl₃-EmimF (molar ratio 2.7) is a one-step three-electron transfer and irreversible diffusion-controlled process. The chronoamperometry results show that the deposition of aluminum on a Pt electrode involves instantaneous three-dimension nucleation. In addition, X-ray diffraction (XRD) analysis confirmed that the deposit is pure aluminum, while scanning electron microscope (SEM) images reveal that dense and compact deposits were obtained at a more negative potential.

1. INTRODUCTION

Hall-Heroult process is the primary and conventional process of producing aluminum from alumina in a high temperature (920–960℃) cryolite-based electrolysis cell, which results in high energy consumption (12.9–13.4 kWh/kg aluminum) and the emission of abundant greenhouse gases such as CO_x (CO, CO_2) and perfluorinated compounds (CF_4, C_2F_6). Meanwhile, the current industrial aluminum electro-refining process such as the three-layer process (Hoope's process) and the

segregation process also has disadvantages of high temperature (800–950 ℃) and high energy consumption (15–18 kWh/kg aluminum) [1].

Thus, it is attractive to develop a more energy-efficient and environmentally friendly process for aluminum extraction and refining. Room temperature ionic liquids are potential electrolyte candidates due to their unique physicochemical properties including low vapor pressure, low melting point, wide electrochemical window and high ionic conductivity. In the last two decades, many researchers have investigated electrodeposition of aluminum or alloys in different ionic liquids[2-18]. Most of researches focused on a mixture of $AlCl_3$ and imidazolium chloride with different substituents due to its adjustable Lewis acidity, appropriate electrochemical widow and high conductivity.

In our previous study, a novel ionic liquid, 1-ethyl-3-methylimidazolium fluoride (EmimF) was synthesized and its properties were investigated [19]. We proposed the possibility of the deposition of aluminum or alloys in 1-ethyl-3-methylimidazolium fluoride ionic liquid. In this study, the aluminum electrodeposition in ionic liquid $AlCl_3$-EmimF was investigated for the first report. The discovery of novel ionic liquid for metal electrodeposition would promote the practical application in various fields. Cyclic voltammetry (CV) and chronopotentiometry were performed to study the electrochemical behavior of $Al_2Cl_7^-$ species in $AlCl_3$-EmimF melts. Additionally, chronoamperometry was carried out to study the nucleation and growth mechanism of aluminum deposits which were characterized by X-ray diffraction and scanning electron microscopy.

2. EXPERIMENTAL

High-purity EmimF was synthesized by mixing and refluxing EmimCl (99%, Lanzhou Institute of Chemical Physics, Lanzhou, China) and silver fluoride (AgF, Aldrich, 98%) at 55–60℃. The reaction of synthesizing EmimF can be expressed as Equation (1). The $AlCl_3$-EmimF ionic liquids were prepared by slowly adding $AlCl_3$ to EmimF in a quartz crucible with continuous stirring under high-purity argon atmosphere in a glove box.

$$EmimCl + Ag = EmimF + AgCl \tag{1}$$

Electrochemical experiments were carried out in a three-electrode cell. Aluminum wire (99.9999%) was used as the reference electrode, while platinum wire (99.99%) with diameter of 0.04 mm was used as the working and counter electrodes. Cyclic voltammetry, chronopotentiometry, and chronoamperometry measurements were performed with an Autolab (PGSTAT30, Metrohm, Netherlands) instrument controlled by GPES software.

All the electrodeposition experiments were conducted in a three-electrode system with a copper sheet (10×20 mm) as the cathode. After electrodeposition, all samples were washed with acetone to remove the electrolyte from the cathode surface and then dried before characterization. The crystal structure of the aluminum deposits were analyzed with X-ray diffraction (XRD, PW3040/60, PANalytical, Netherlands). The surface morphologies of the aluminum coatings were performed with scanning electron microscopy (SEM, SSX-550, Shimadzu Corp., Japan).

3. RESULTS AND DISCUSSION

3.1 Cyclic voltammetry

To investigate the electrochemical behavior of aluminum species, CV was carried out in $AlCl_3$-EmimF (molar ratio 2.7) on a Pt electrode at 90℃. As shown in Figure 1A, a cathodic current with an onset potential at –0.1 V was observed, while a corresponding anodic peak was observed at 0.55V (Peak B). In addition, the coating obtained on the copper sheet by constant potential electrolysis at –0.3 V was confirmed to be metallic aluminum by XRD. It has been reported that the acid electrolyte of $AlCl_3$-EmimCl (or BmimCl) mainly contains $Al_2Cl_7^-$, along with minor $AlCl_4^-$ and $Al_3Cl_{10}^-$ ions [2]. Therefore, aluminum deposition in $AlCl_3$-EmimF (molar ratio 2.7) is ascribed to the reduction of $Al_2Cl_7^-$ ions that are abundant in the acid melts. Corresponding reactions to Peaks A and B are given by Equations (2) and (3). Additionally, the anodic peak at 2.2 V is associated with the oxidation of the $AlCl_4^-$ anion (as shown in Equation (4)).

$$4Al_2Cl_7^- + 3e = Al + 7AlCl_4^- \tag{2}$$

$$Al + 7AlCl_4^- - 3e = 4Al_2Cl_7^- \tag{3}$$

$$4Al_2Cl_7^- - 2e = 2AlCl_4^- + Cl_2 \tag{4}$$

Figure 1B presents the CVs recorded on the Pt working electrode in $AlCl_3$-EmimF (molar ratio 2.7) at different scan rates. The cathodic peak potential shifts negatively with the increase of the scan rate, while the anodic peak potential shifts positively with increasing of the scan rate. Additionally, the separation between the cathodic and anodic peak potentials is as large as 500 mV. Furthermore, as seen in Figure 1C, the reduction current of the peak (I_{pc}) is linearly related with the square root of the scanning rate ($v^{1/2}$), which is a characteristic of the Randles-Sevcik equation [20]. Therefore, the reduction of $Al_2Cl_7^-$ to metallic Al in $AlCl_3$-EmimF (molar ratio 2.7) is an irreversible diffusion-controlled process [21]. For an irreversible charge transfer process, the number of exchanged electrons can be calculated as follows [22]:

$$E = B - \frac{RT}{nF} \ln \frac{I}{I_p - I} \tag{5}$$

where E is the potential, B is the half-wave potential, R is the universal gas constant (8.314 J·K^{-1}·mol^{-1}), T is the experimental temperature, n is the number of transferred electron, F is the Faraday constant (96500 C·mol^{-1}), I is the current, and I_p is the maximum current. The relationship between E and ln [($I/(I_p$ -I)] in Figure 1B at scan rate of 0.1 V/s is shown in Figure 1D. Thus, the computed value of n is 3.006, close to three electrons, which is in good agreement with the reaction shown in Equation (2). That is to say, the reduction of $Al_2Cl_7^-$ to metallic aluminum in $AlCl_3$-EmimF (molar ratio 2.7) is an irreversible diffusion-controlled process and it proceeds via a one-step three-electron transfer process.
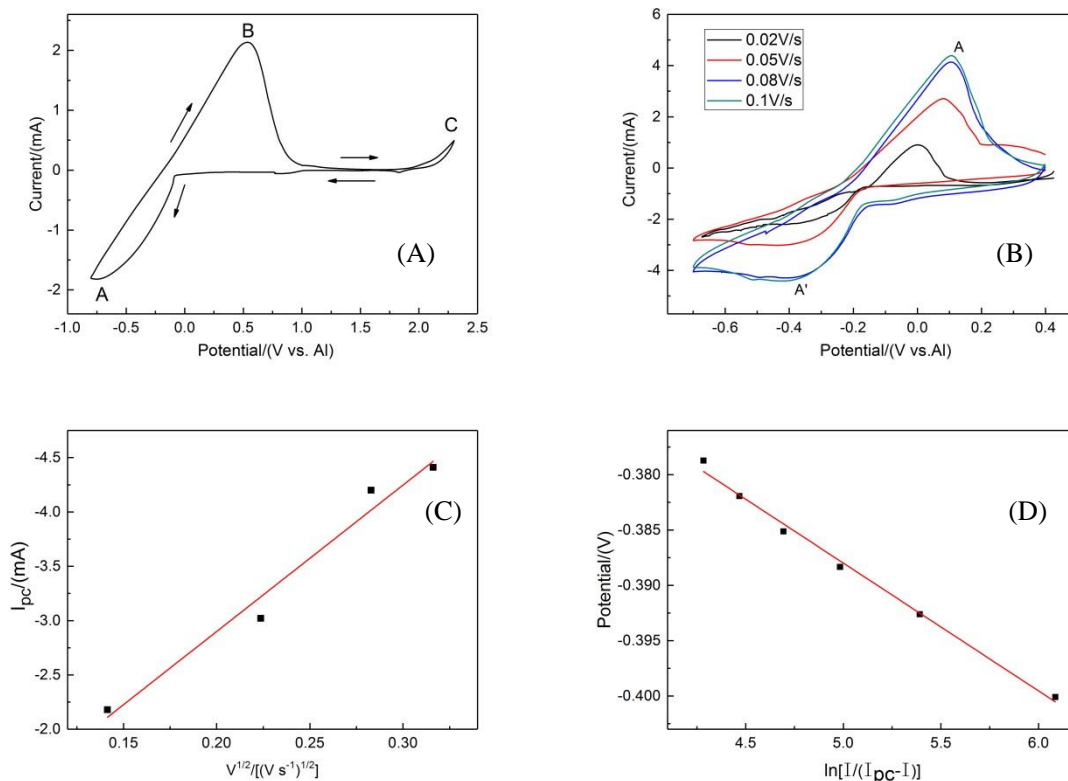
Figure 1. (A) CV curve of Pt electrode in AlCl$_3$-EmimF (molar ratio 2.7) at 90 °C（vs. Al/AlCl$_3$ reference electrode, Scan rate 0.08 V/s). (B) CV curves of Pt electrode in AlCl$_3$-EmimF (molar ratio 2.7) at 90 °C under different scan rates. (C) Relationship of Al$_2$Cl$_7^-$ reduction peak current versus the square root of the scan rate. (D) Relationship between potential and ln [(I/(I_p -I)] at scan rate of 0.1 V/s in AlCl$_3$-EmimF (molar ratio 2.7).
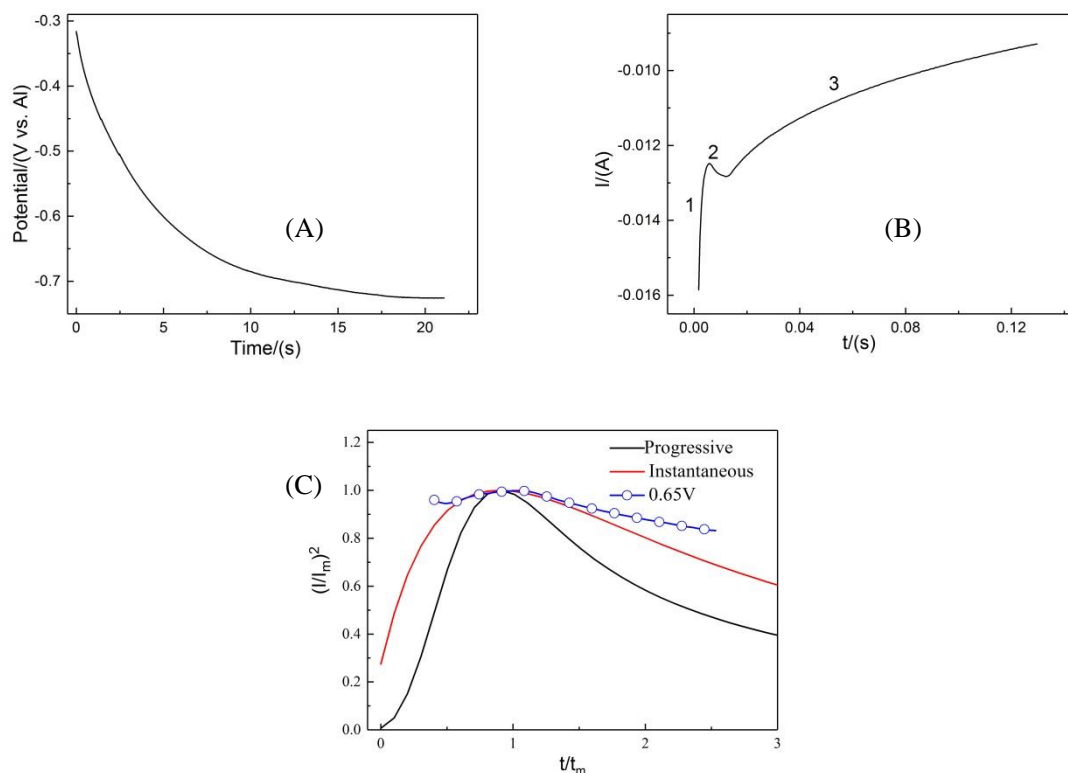
3.2 Chronopotentiometry and Chronoamperometry

As shown in Figure 2A, the analysis by chronopotentiometry of AlCl$_3$-EmimF (molar ratio 2.7) showed the existence of one potential plateau in the potential range between –0.32 and –0.73V. The plateau at –0.73V is associated with the reduction of Al$_2$Cl$_7^-$ to aluminum, and it proceeds by a one-step process, which agrees well with the result and discussion from Figure 1.

Chronoamperometry was performed on a Pt electrode to study the nucleation and growth mechanism of aluminum deposits in AlCl$_3$-EmimF (molar ratio 2.7). A typical current-time transient curve obtained at –0.65V is shown in Figure 2B. After the decay of a sharp Pt electrode double layer charging current, the subsequent increasing of current (peak current maximum, i$_m$) was observed due to the nucleation and growth of aluminum nuclei. The following current showed transient decay slowly at time t$_m$ because of the increased diffusion layer thickness and overlap of the nucleus which reduced the activity of the atom incorporation into the crystal lattice. Scharifker et al. described the nucleation and growth mechanism of metal nuclei either by instantaneous nucleation or progressive nucleation model [23-24]. To determine the nucleation and growth mechanism of aluminum in AlCl$_3$-EmimF, the data from Figure 2B is compared with the theoretical instantaneous (Equation (6)) and progressive (Equation (7)) nucleation processes. It was represented in Figure 2C that the experimental result was in

close agreement with the instantaneous three-dimension nucleation defined by Equation (6). Therefore, the electrodeposition of aluminum in $AlCl_3$-EmimF can be considered as instantaneous three-dimension nucleation under diffusion control.

$$\left(\frac{I^2}{I_m^2}\right) = 1.9542 \left(\frac{t}{t_m}\right)^{-1} \left\{1 - \exp\left[-1.2564\left(\frac{t}{t_m}\right)\right]\right\}^2 \tag{6}$$

$$\left(\frac{I^2}{I_m^2}\right) = 1.2254 \left(\frac{t}{t_m}\right)^{-1} \left\{1 - \exp\left[-2.3367\left(\frac{t}{t_m}\right)^2\right]\right\}^2 \tag{7}$$

Figure 2. (A) Chronopotentiogram of $AlCl_3$-EmimF (molar ratio 2.7) at current of 3 mA. (B) Current density-time transients of chronoamperometric experiments for $AlCl_3$-EmimF (molar ratio 2.7) on Pt electrode. (C) Comparison of the dimensionless current density-time transients of chronoamperometric experiments for $AlCl_3$-EmimF (molar ratio 2.7) on Pt electrode with the theoretical models of 3D nucleation at -0.65V.

3.3 Electrodeposition and characterization of deposits

The XRD pattern of the aluminum deposits obtained from $AlCl_3$-EmimF (molar ratio 2.7) at –0.3V is shown in Figure 3D. All peaks in the pattern are associated with Al and the Cu substrate. The peaks of carbon and $AlCl_3$ were not found, which agrees with previous discussions. In addition, the surface morphologies of aluminum obtained at different cathodic potential (–0.2V, –0.3V, –0.4V) for 30 min in $AlCl_3$-EmimF are shown in Figure 3A–C. The grain size decreases with the negative shift of electrodeposition potential. As the nucleation of Al on the Pt electrode is an instantaneous three-dimension nucleation, the classical vapor pressure nucleation theory (Equation (9)) can be used to reveal the relationship between the over-potential and nucleation rate. Thus, increased over-potential

results in the diminishment of the particle size with a greater amount of the nucleus at equal electric quantity.

$$J = A\exp(-B/\eta) \tag{8}$$

where J is the nucleation rate, A is an exponent parameter, η is the over-potential, and B is a parameter that affects crystallization process.
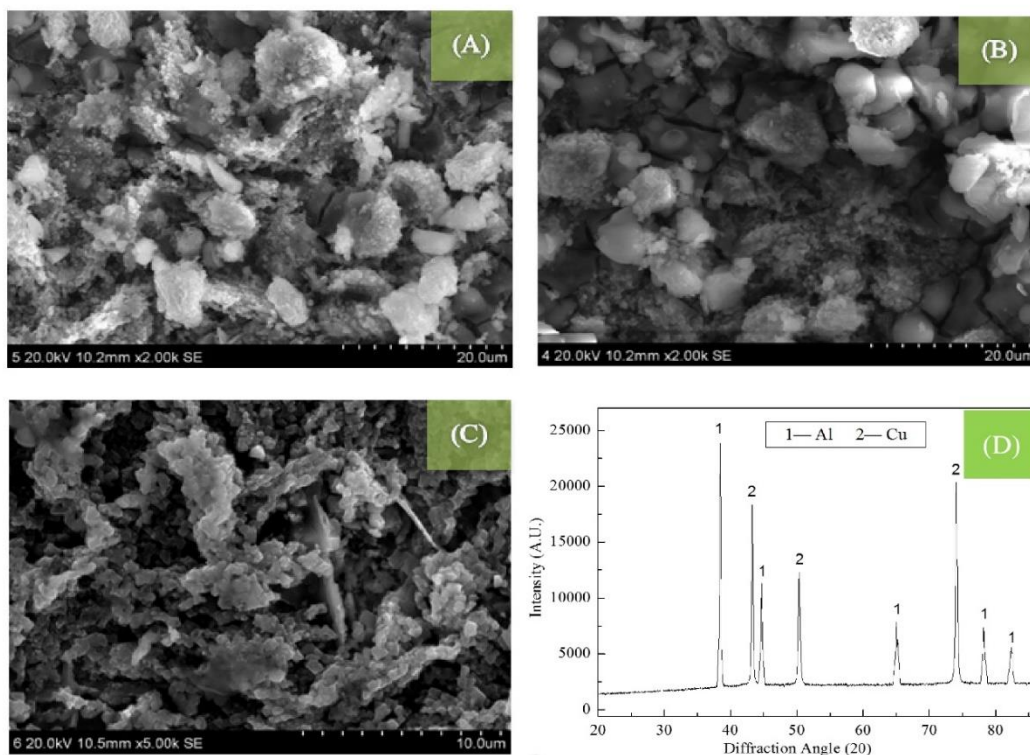
Figure 3. SEM micrographs of Al deposits obtained from AlCl$_3$-EmimF (molar ratio 2.7) at potential of (A) -0.2V, (B) -0.3V, and (C) -0.4V. (D) The XRD pattern of the Al deposits obtained from AlCl$_3$-EmimF at -0.3V.

3.3 Comparation with other systems

As the particular properties of AlCl$_3$, the most electrolytes for electrodeposition were based AlCl$_3$ system as listed in Table 1.

Table 1. Electrodeposition of aluminum or alloys reported in literatures

Ionic Liquids as Electrolytes	Metals or Alloy Electrodeposition	References
AlCl$_3$-1-ethyl-3-methyl-imidazolium chloride (EmimCl)	Al	[2-8]
AlCl$_3$-1-butyl-3-methyl-imidazolium chloride (BmimCl)	Al	[9-10]
AlCl$_3$-acetamide	Al	[11]

AlCl$_3$-trimethylpheneylammonium chloride	Al	[12-14]
AlCl$_3$-1-ethyl-3-methyl-imidazolium chloride (EmimCl)	Al-Ti	[15]
AlCl$_3$-1-ethyl-3-methyl-imidazolium chloride (EmimCl)	Al-Zr	[16]
AlCl$_3$-1-ethyl-3-methyl-imidazolium chloride (EmimCl)	Al-Mo	[17]
AlCl$_3$-1-ethyl-3-methyl-imidazolium chloride (EmimCl)	Al-Mo-Ti	[18]
AlCl$_3$-1-Ethyl-3-Methylimidazolium Fluoride (EmimF)	Al	This work

Jiang et al. [2] and other researchers [3-8] studied the electrodeposition of aluminum in Lewis acidic AlCl$_3$-1-ethyl-3-methyl-imidazolium chloride (EmimCl), and results indicated that thin aluminum deposits (less than 0.2 μm) can be obtained in acidic melts by the reduction of Al$_2$Cl$_7^-$ species. Reddy et al. [9-10] proposed that dendrite-free aluminum can be electrodeposited from AlCl$_3$-1-butyl-3-methyl-imidazolium chloride (BmimCl). Li et al. [11] suggested that compact aluminum coatings on copper cathodic substrate can be obtained from AlCl$_3$-acetamide eutectic solvent. In addition, Zhao et al. [12-13] and Jiang et al. [14] studied the deposition of aluminum from AlCl$_3$-trimethylpheneylammonium chloride and they found that the aluminum deposition was a diffusion controlled instantaneous three-dimension nucleation. On the other hand, the Lewis acidic AlCl$_3$-EmimCl was also applied to the production of aluminum alloys such as Al-Ti[15], Al-Zr[16], Al-Mo[17], and Al-Mo-Ti [18]. In this work, we obtained the aluminum metal in a novel ionic liquids system, AlCl$_3$-EmimF, as the electrolyte. The solubility and electrodeposition of other metals in this system could be studied in the future research.

4. CONCLUSION

Aluminum was successfully prepared in AlCl$_3$-EmimF at a potential of –0.3V (vs. Al/Al^{3+}) and temperature of 90 ℃. The electrochemical behavior of Al$_2$Cl$_7^-$ was investigated by cyclic voltammetry, chronopotentiometry, and chronoamperometry. Cyclic voltammetry and chronopotentiometry indicate that the reduction of Al$_2$Cl$_7^-$ to metallic Al on a Pt electrode in AlCl$_3$-EmimF (molar ratio 2.7) is an irreversible diffusion-controlled process and it proceeds via a one-step three-electron transfer process. Chronoamperometry show that the deposition of aluminum in AlCl$_3$-EmimF involves instantaneous three-dimension nucleation. In addition, the deposits were characterized by XRD and SEM. XRD analysis confirmed that the deposit is pure aluminum. SEM images reveal that dense and compact deposits were obtained at a more negative potential.

References

1. M. Kondo, H. Maeda and M. Mizuguchi, *JOM,* 42 (1990) 36.
2. T. Jiang, M. J. C. Brym, G. Dube, A. Lasia and G.M. Brisard, *Surf. Coat. Technol.*, 201 (2006)1.

3. Q. X. Liu, S. Z. E. Abedin and F. Endres, *Surf. Coat. Technol.,* 201(2006)1352.
4. S. Z. E. Abedin, P. Giridhar, P. Schwab and F. Endres, *Electrochem. Commun.*, 12 (2010)1084.
5. B. Li, C.H. Fan, Y. Chen, J.W. Lou and L.G. Yan, *Electrochim. Acta,* 56 (2011)5478.
6. L. H. S. Gasparotto, A. Prowald, N. Borisenko, S. Z. E. Abedin, A. Garsuch and F. Endres, *J. Power Sources,* 196 (2011)2879.
7. A. Bakkar and V. Neubert, *Electrochim. Acta,* 103 (2013) 211.
8. A. Bakkar and V. Neubert, *Electrochem. Commun.*, 51 (2015)113.
9. V. Kamavaram, D. Mantha and R.G. Reddy, *J. Min. Metall. Sect. B.*, 39(2003)43.
10. D. Pradhan and R. G. Reddy, *Mater. Chem. Phys.,* 143(2014)564.
11. M. Li, B. L. Gao, C.Y. Liu, W. T. Chen, Z.N. Shi, X. W. Hu and Z. W. Wang, *Electrochim. Acta,* 180 (2015)811.
12. Y. G. Zhao and T. J. V. Noot, *Electrochim. Acta,* 42(1997)1639.
13. Y.G. Zhao and T. J. V. Noot, *Electrochim. Acta,* 42(1997)3.
14. T. Jiang, M. J. C. Brym, G. Dube, A. Lasia and G.M. Brisard, *Surf. Coat. Technol.*, 201(2006)10.
15. T. Tsuda, C. L. Hussey, G. R. Stafford and J. E. Bonevich, *J. Electrochem. Soc.*, 150(2003)C234.
16. T. Tsuda, C. L. Hussey, G. R. Stafford and O. Kongstein, *J. Electrochem. Soc.*, 151(2004)C447.
17. T. Tsuda, C. L. Hussey and G. R. Stafford, *J. Electrochem. Soc.*, 151(2004)C379.
18. T. Tsuda, S. Arimoto, S. Kuwabata and C. L. Hussey, *J. Electrochem. Soc.*, 155(2008)D256.
19. F. Liu, X. Zhong, J. Xu, A. Kamali and Z. Shi, *Appl. Sci.,* 8(2018)356.
20. Z. N. Shi, M. Li, L. L. Li, B. L. Gao, X. W. Hu and Z. W. Wang, *Trans. Nonferrous Met. Soc. China*, 21(2011)1655.
21. A. M. Liu, Z. N. Shi, J. L. Xu, X. W. Hu, B. L. Gao and Z. W. Wang, *JOM,* 68(2016)1518.
22. A. J. Bard, and R. L. Faulkner, *Electrochemical methods fundamentals and applications*, 2 nd ed. p. 231-232,: John Wiley & Sons, Inc., New York, (2001).
23. G. Gunawardena, G. Hills, I. Montenegro and B. Scharifker, *J. Electroanal. Chem.*, 138(1982)225.
24. B. Scharifker and G. Hills, *Electrochim. Acta,* 28(1983)879.